Journal of Power Sources 216 (2012) 89–98

Contents lists available at SciVerse ScienceDirect

Journal of Power Sources

journal homepage: www.elsevier.com/locate/jpowsour

Chromium poisoning and degradation at $Gd_{0.2}Ce_{0.8}O_2$-impregnated $LaNi_{0.6}Fe_{0.4}O_{3-\delta}$ cathode for solid oxide fuel cell

Bo Huang*, Xin-jian Zhu, Rui-xuan Ren, Yi-xing Hu, Xiao-yi Ding, Ye-bin Liu, Zong-yao Liu

Institute of Fuel Cell, School of Mechanical Engineering, Shanghai Jiaotong University, 800 Dongchuan Road, Shanghai 200240, PR China

HIGHLIGHTS

- R_p increases with time to the power of 1/3 and 1/5 in LNF and 21.3 wt.%GDC-impregnated LNF under Cr exposure.
- LNF exhibits far greater R_p than that of 21.3 wt.%GDC-impregnated LNF under Cr exposure.
- No significant degradation in performance is observed under Cr exposure in 21.3 wt.%GDC-impregnated LNF.

ARTICLE INFO

Article history:
Received 16 March 2012
Received in revised form
18 May 2012
Accepted 21 May 2012
Available online 28 May 2012

Keywords:
Chromia-forming alloy
Chromium poisoning
Electrochemical properties
Impedance spectroscopy
Oxygen reduction
Solid oxide fuel cell

ABSTRACT

The degradation of cathode performances by chromium poisoning is studied at two cathodes $LaNi_{0.6}Fe_{0.4}O_{3-\delta}$ (LNF) and 21.3 wt.% $Gd_{0.2}Ce_{0.8}O_2$ (GDC)-impregnated $LaNi_{0.6}Fe_{0.4}O_{3-\delta}$ on the scandia stabilized zirconia (ScSZ) electrolyte. Specific polarization resistance (R_p) increases with time to the power of 1/3 and 1/5 in LNF and 21.3 wt.% GDC-impregnated LNF cathode after operating under a cathodic current density of 50 mA cm^{-2} under exposure of Cr vapors at 750 °C for 370 h and 1042 h, respectively. electrochemical impedance spectroscopy (EIS) illustrate that LNF exhibits far greater R_p than that of 21.3 wt.%GDC-impregnated LNF under exposure of Cr vapors due to strong Cr deposition at LNF/ScSZ interface. No significant degradation in performance has been observed after 1042 h of operating under a cathodic current density of 50 mA cm^{-2} under exposure of Cr vapors at 750 °C due to very little Cr deposition at 21.3 wt.%GDC-impregnated LNF/ScSZ interface, suggesting little poisoning effect for O_2 reduction on 21.3 wt.%GDC-impregnated LNF cathode. The results demonstrate that 21.3 wt.%GDC-impregnated LNF cathode has a high resistance toward Cr deposition and high tolerance toward Cr poisoning.

1. Introduction

Solid oxide fuel cell (SOFC) will inevitably exert a great impact on the development of the next generation energy technology and the hydrogen economy due to their high energy conversion efficiency, fuel flexibility, use of non-noble and cost-effective electrodes, and production of high quality waste heat. For example, the efficiency of the SOFC systems can be further increased when the SOFC systems are combined with the gas turbine or steam turbine to provide additional power [1]. Intermediate-temperature solid oxide fuel cell (IT-SOFC) has currently received much attention. The lower operating temperature allows the use of metallic materials as the interconnects. Nowadays, most widely used interconnects are the Cr-containing steels due to their high thermal and electronic conductivity, good machineability, matching thermal expansion coefficient to the ceramic cell components and low material cost [2–5]. However, the application of the Cr-containing alloys still poses many challenges even at reduced temperatures. For instance, at elevated temperature, a layer of chromium oxide (Cr_2O_3) formed on the surface of the Cr-containing alloy interconnect after long-time exposure to the SOFC environment results in high electrical resistance which degrades cell performance [3,6]. Furthermore, on the cathode side, Cr_2O_3 can react with oxygen and moisture to form volatile Cr species in oxidizing atmospheres under SOFC operating temperatures [7–9]. Das et al. [10] have also systematically studied, by thermodynamic computations, the vaporisation of Cr volatile species above the Fe–Cr alloy in dry and moist air as functions of oxygen partial pressure and temperature. A number of volatile Cr species can form over Cr_2O_3(s) due to reaction with oxygen. Among several kinds of Cr gas phases, CrO_3 and $CrO_2(OH)_2$ are considered as high vapor pressure phases [9,11]. At low humidity, CrO_3(g) is the main gas species described as

$$Cr_2O_3(s) + 3/2O_2(g) \rightarrow 2CrO_3(g) \quad (1)$$

* Corresponding author. Tel./fax: +86 21 34206249.
E-mail address: huangbo2k@hotmail.com (B. Huang).

0378-7753/$ – see front matter © 2012 Elsevier B.V. All rights reserved.
doi:10.1016/j.jpowsour.2012.05.058

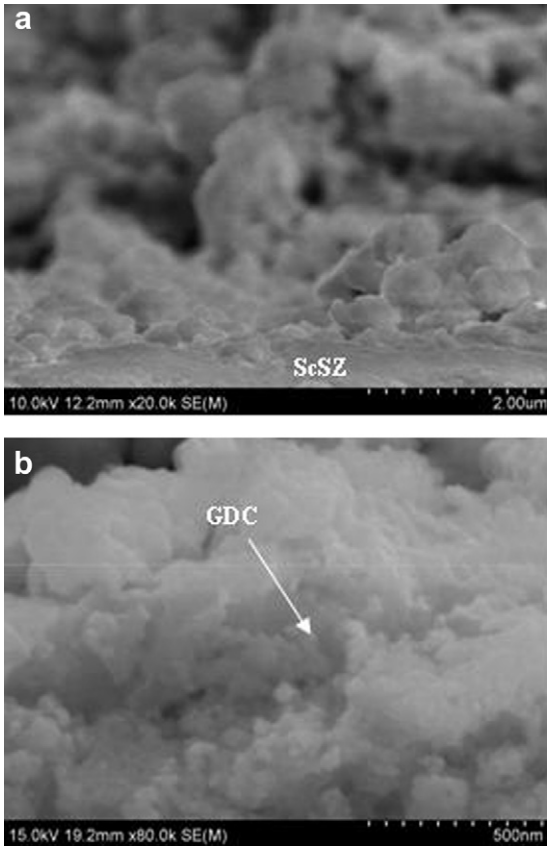

Fig. 1. Scanning electron microscope images of the fractured cross section of LNF (a) and 21.3 wt.% GDC-impregnated LNF (b) cathodes before Cr-poisoning test.

In the presence of moisture and oxygen, as may often be the case in single cell due to the presence of normal moisture levels in air, a number of $CrO_2(OH)_2$ can also exist above $Cr_2O_3(s)$ as the following reaction

$$1/2Cr_2O_3(s) + H_2O(g) + 3/4O_2(g) \rightarrow CrO_2(OH)_2(g) \quad (2)$$

Thus a number of Cr(6+) species such as $CrO_3(g)$ and $CrO_2(OH)_2(g)$ have significant vapor pressure above $Cr_2O_3(s)$ in moist air. These species would freely move around. A sufficient quantity would migrate through the porous structure of the cathode and reach the cathode/electrolyte interface. The normal process at the cathode/electrolyte interface is the O_2 reduction reaction $O_2 + 4e^- \rightarrow 2O^{2-}$, but dissociation of water (in a steam electrolyzer, based on oxygen-ion conducting electrolyte) also occurs (via the reaction: $H_2O(g) + 2e^- \rightarrow H_2(g) + O^{2-}$) on application of a negative bias at the cathode/electrolyte interface. Similarly, other oxides in the vapor form which can supply oxygen at the interface can be easily reduced. Thus, when $CrO_2(OH)_2$ and CrO_3 reach the oxide ion-conducting media (electrolyte) and an electrically conducting phase (cathode), the following reactions for $CrO_2(OH)_2(g)$ and $CrO_3(g)$ are likely to compete with the normal O_2 reduction process [12]:

$$2CrO_3(g) + 6e^- \rightarrow Cr_2O_3(s) + 3O^{2-} \quad (3)$$

$$2CrO_2(OH)_2(g) + 6e^- \rightarrow Cr_2O_3(s) + 2H_2O(g) + 3O^{2-} \quad (4)$$

Cr^{6+} can be readily reduced to Cr^{3+}, electrochemically forming Cr_2O_3 and releasing water and an oxide ion at the cathode/electrolyte interface. Therefore, in the case of $CrO_2(OH)_2(g)$ and $CrO_3(g)$, unlike the O_2 reduction reaction, a significant amount of residue in the form of $Cr_2O_3(s)$ is left behind at the cathode/electrolyte interface. Another possible cause for $Cr_2O_3(s)$ deposition at the cathode/electrolyte interface may be indirectly related to the oxygen reduction reaction [12,13]. Since the reaction $2CrO_3(g) \rightarrow Cr_2O_3(s) + 1.5O_2$ is driven by the oxygen partial pressure at a constant temperature, the deposition of $Cr_2O_3(s)$ at or near the interface can also occur due to the lower oxygen partial pressure at the cathode/electrolyte interface compared to that in the bulk gas phase, which is also possible in a cell polarized with large current densities. The accumulation of chromium oxide contaminants, eventually leads to cathodic polarization loss and to rapid performance degradation of the SOFC [7,9,14–17], which has been reported as "Cr poisoning" that is one of the critical issues among several degradation factors of cathode in SOFC [18].

Cr poisoning is most significant in the $(La,Sr)MnO_3$ cathode because the electrochemical active parts are limited to the gas/cathode/electrolyte interfaces (TPB). It is also reported that the deposition process is essentially dominated by the chemical dissociation of the gaseous Cr species, and is most likely limited by the nucleation reaction between these Cr species and the nucleation agents such as manganese species (Mn^{2+}) generated from $(La,Sr)MnO_3$ under the cathodic polarization in the $(La,Sr)MnO_3$ cathode-zirconia electrolyte system [19]. Mn^{2+} ions on the $(La,Sr)MnO_3$ surface can react with the Cr species and forms the Cr–Mn–O nuclei and, subsequently, $(Cr,Mn)_3O_4(s)$ [12, 20]. The chemical reaction of Cr with $(La,Sr)CoO_3$ is significant to form $SrCrO_4$ on the porous $(La,Sr)CoO_3$ surface [15,21–22]. The formation rate of $SrCrO_4$ is different depending on the chemical affinity of cathode materials, especially B-site in the ABO_3 perovskite structure: $(La,Sr)CoO_3$ is more reactive than $(La,Sr)MnO_3$. The effects of the B-site and Sr activity in perovskites on the reactivity with Cr have also been estimated by the

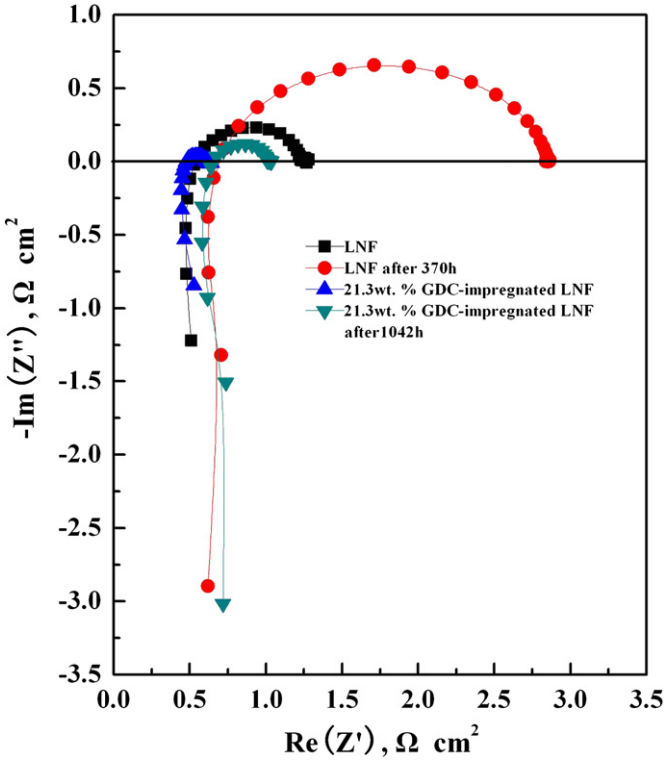

Fig. 2. Electrochemical impedance spectra of LNF and 21.3 wt.%GDC-impregnated LNF cathodes under a cathodic current density of 50 mA cm^{-2} without Cr vapors at 750 °C during the aging process.

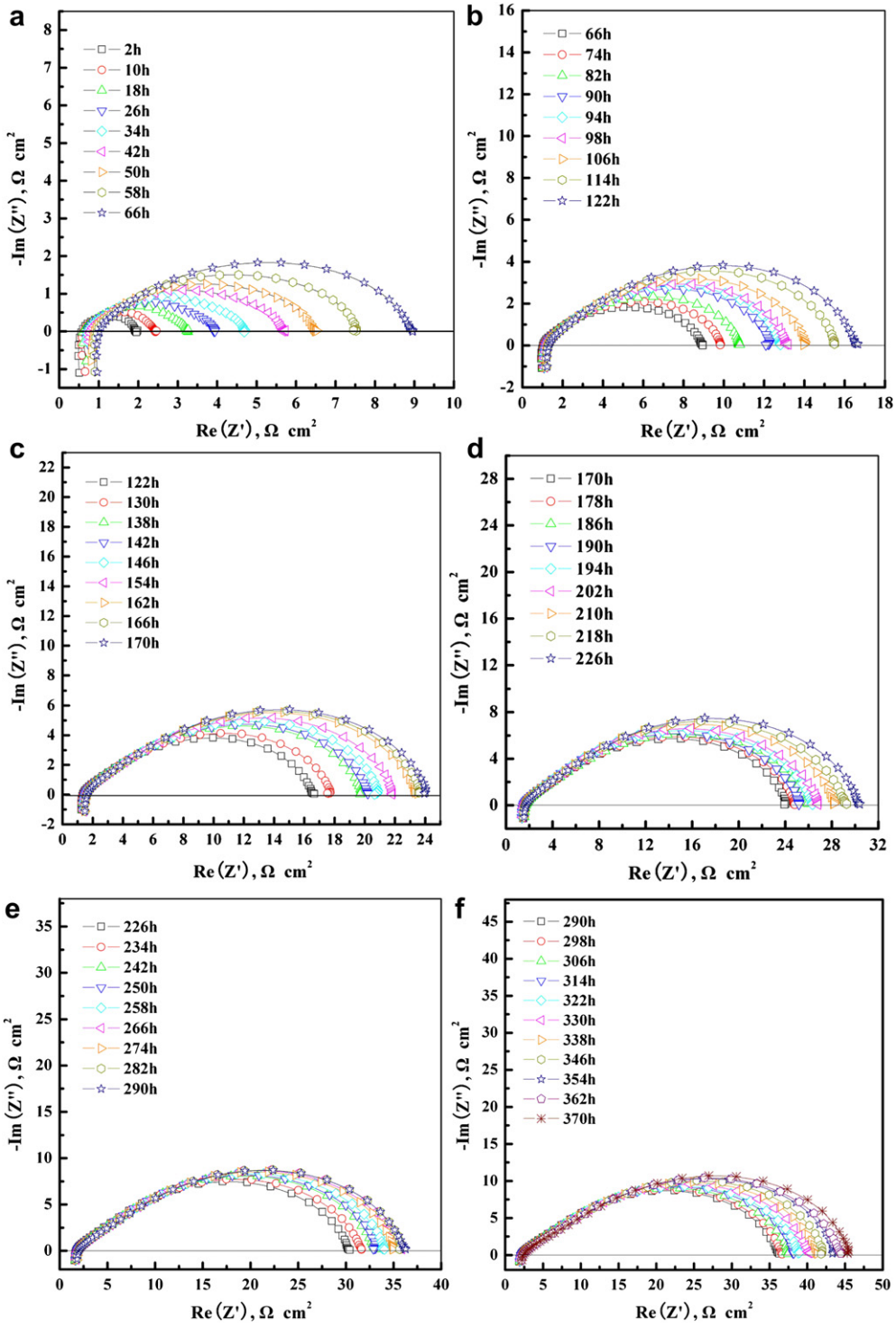

Fig. 3. Electrochemical impedance spectra of the LNF cathode under a cathodic current density of 50 mA cm^{-2} under exposure of Cr vapors at 750 °C during the aging process.

thermodynamic calculation [16]: There is a clear difference in stability against the Cr species with different perovskites. Systematic studies have also shown that the interaction between the Cr species and cathodes is strongly dependent on the nature of the cathode materials [23], which suggests the possibility to develop stable cathode materials with high tolerance to Cr poisoning by proper modification of the conventional (La,Sr)MnO_3 cathode material or cathode composition, i.e., without a nucleation agent for Cr deposition. Although numerous approaches to add protective coatings on the metallic interconnect have been explored, the application of protective coating layers seems to be questionable due to high costs, comparatively low electronic conductivities and difficulties with the fabrication of dense coating layers [11,24–28].

La(Ni,Fe)O_3 perovskite material has been developed as one of the most promising cathode materials because of its high electronic conductivity, thermal expansion coefficient close to that of the zirconia electrolyte and high electrochemical activity for the oxygen reduction reaction [29–32]. It has also recently been found that

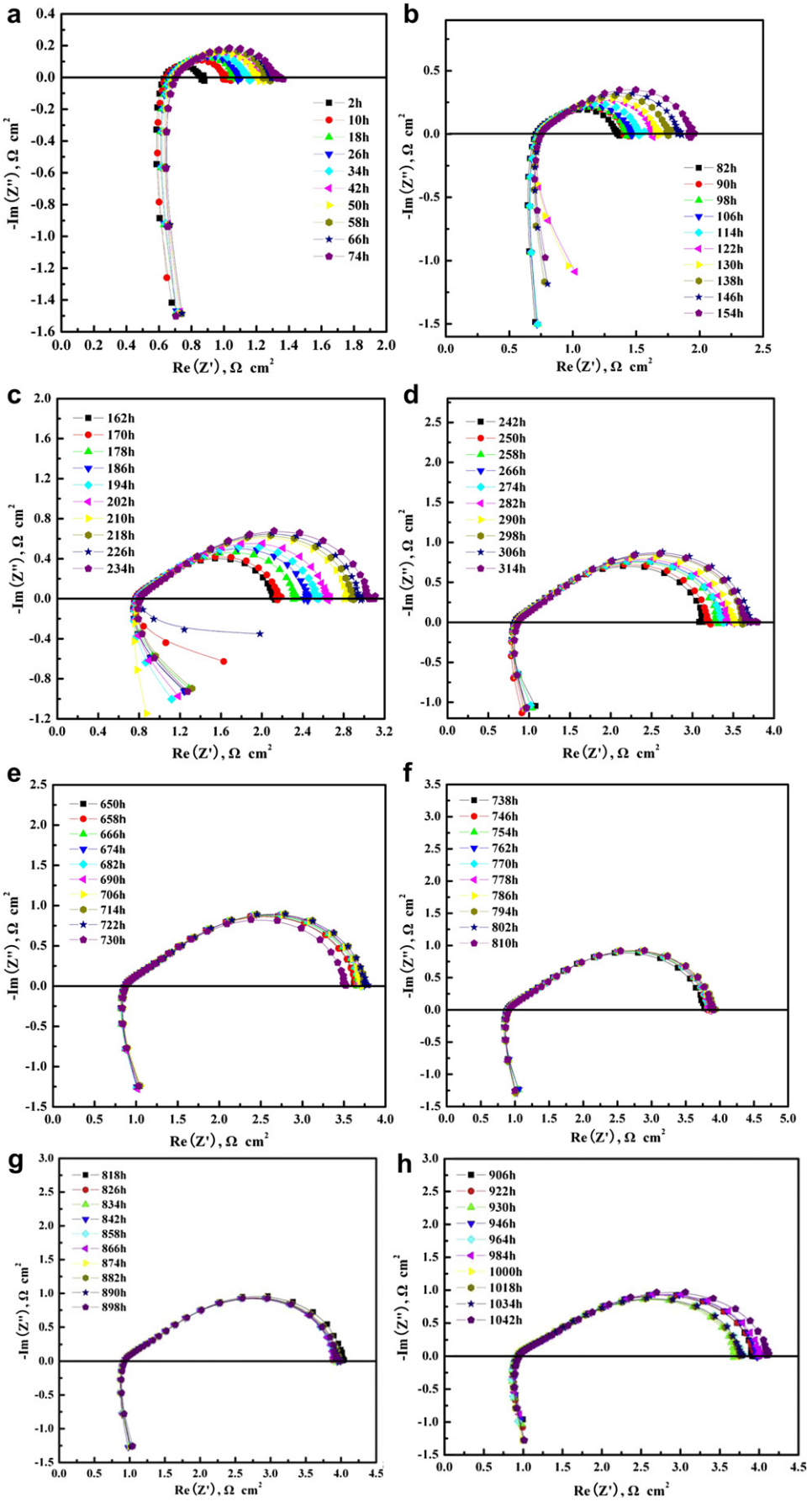

Fig. 4. Electrochemical impedance spectra of 21.3 wt.%GDC-impregnated LNF cathode under a cathodic current density of 50 mA cm^{-2} under exposure of Cr vapors at 750 °C during the aging process.

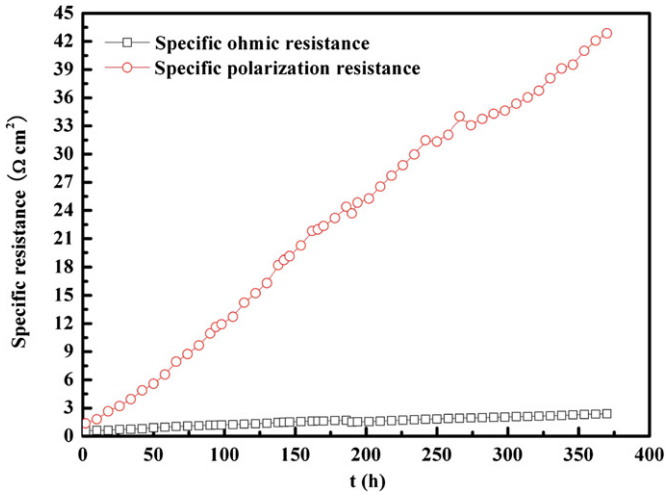

Fig. 5. Evolution of the specific polarization resistance and the specific ohm resistance of the $LaNi_{0.6}Fe_{0.4}O_{3-\delta}$ cathode under a cathodic current density of 50 mA cm^{-2} under exposure of Cr vapors at 750 °C during the aging process.

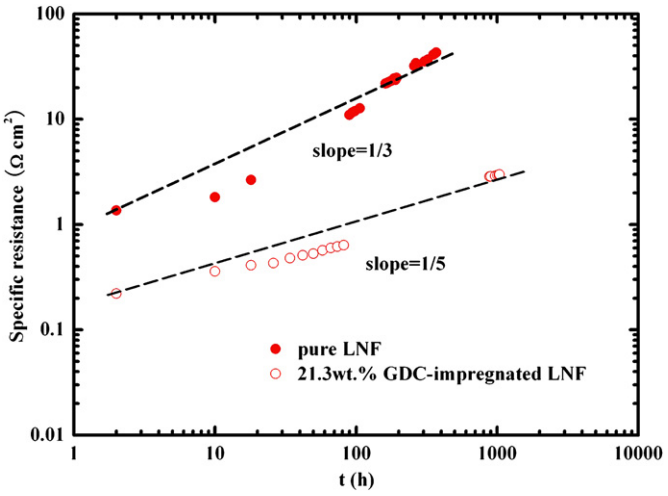

Fig. 7. Specific polarization resistance change with time for pure LNF and 21.3 wt.% GDC-impregnated LNF cathode under a cathodic current density of 50 mA cm^{-2} under exposure of Cr vapors at 750 °C during the aging process.

La(Ni,Fe)O_3-based cathodes have higher resistance to chromium poisoning [33,34]. However, recent endurance test data obtained at ECN on SOFCs with an La(Ni,Fe)O_3-based cathode at operating temperatures of 800–850 °C, showed degradation in cell performance when tested in combination with a chromium containing metallic interconnect [35], despite the claimed Cr-resistance of La(Ni,Fe)O_3-based cathode in the literature. Further studies have also found that vapor transport of Cr species, originating from a porous metallic foam, and subsequent reaction with La(Ni,Fe)O_3, results in the decrease of the electronic conductivity of the La(Ni,Fe)O_3 layer, and the increase of the polarization resistance of the La(Ni,Fe)O_3 cathode [36,37]. Therefore, further improvement in the performance of the La(Ni,Fe)O_3 cathode is required. Optimization of the microstructure of the La(Ni,Fe)O_3-based cathode with respect to lateral conductivity and three phase boundaries (TPB) at the cathode/electrolyte interface, has been shown to result in enhanced electrochemical performance [38]. In order to improve the performance of $LaNi_{0.6}Fe_{0.4}O_{3-\delta}$, $Ce_{0.9}Gd_{0.1}O_{2-\alpha}$ powder was added by ball milling to prepare the $LaNi_{0.6}Fe_{0.4}O_{3-\delta}$-$Ce_{0.9}Gd_{0.1}O_{2-\alpha}$ (LNF-CGO) composite cathode [39]. The result indicated that the added CGO slightly improved the resistance toward Cr deposition of the LNF cathode after 200 h. The performance after much longer time has not yet been reported. To estimate the long-term durability of the La(Ni,Fe)O_3 cathode, it is important to know the amounts of Cr in the cathode and the effects of Cr poisoning on the cathode performance and degradation. In this paper, the fabrication and cathode behavior of the $Gd_{0.2}Ce_{0.8}O_2$ (GDC)-impregnated La(Ni,Fe)O_3-based cathode have been investigated. The electrochemical performance of the cathode for oxygen reduction is systematically investigated in the presence of the chromia-forming alloy interconnect during the aging process. The results indicate that the impregnation of GDC phase not only substantially enhances the performance of the La(Ni,Fe)O_3-based cathode associated with the O_2 reduction reaction, but also substantially improves the Cr-poisoning resistance of the La(Ni,Fe)O_3-based cathode in the presence of the chromia-forming alloy interconnect.

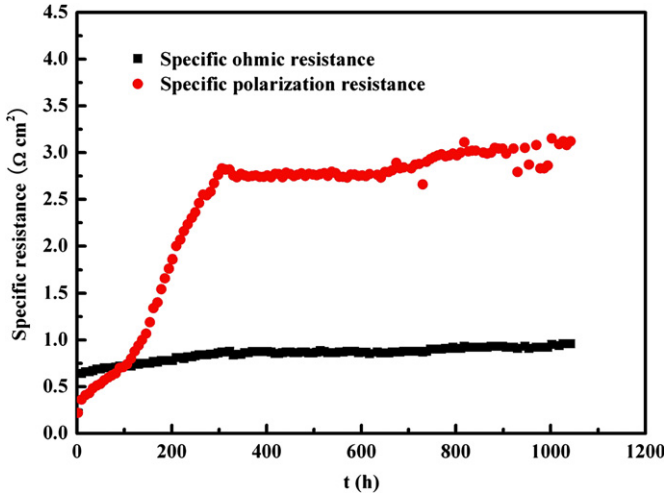

Fig. 6. Evolution of the specific polarization resistance and the specific ohm resistance of 21.3 wt.%GDC-impregnated LNF cathode under a cathodic current density of 50 mA cm^{-2} under exposure of Cr vapors at 750 °C during the aging process.

2. Experimental

2.1. Preparation of GDC-impregnated LNF cathode

The composition of La(Ni,Fe)O_3-based cathode was chosen as $LaNi_{0.6}Fe_{0.4}O_{3-\delta}$ (LNF) [20,21]. The LNF cathode material was prepared using a combustion synthesis technique described elsewhere [40]. The polarization resistance of the $LaNi_{0.6}Fe_{0.4}O_{3-\delta}$ cathode was measured in the two-electrode symmetric cell configuration under air [41]. ScSZ (scandia stabilized zirconia, $Sc_{0.1}Zr_{0.9}O_{1.95}$, 99.99% pure, Daiichi Kigenso, Japan) pellet with the diameter of 20 mm and the thickness of about 200 μm was used as the electrolyte. Electrolyte-supported symmetric cell for impedance testing was fabricated by screen printing method. The slurry of the LNF cathode powder, which was ground and mixed with isopropyl alcohol, was screen-printed onto both sides of the ScSZ electrolyte pellet. Then the symmetric cell was sintered at 1050 °C for 2 h under stagnant air. After being sintered, the resulting LNF cathode areas are 1 cm^2. The LNF cathode is a square in shape. The side length of the square is 1 cm. GDC ($Gd_{0.2}Ce_{0.8}O_2$)-impregnated LNF cathode was prepared according to reference [40]. Field emission scanning electron microscope (FE-SEM) images of the interface layer GDC-impregnated LNF/ScSZ before and after Cr-poisoning test were analyzed using a microscope (FE-SEM, PHILIPS 515, Holland) equipped with an X-ray analyzer for energy-dispersive X-ray spectroscopy (EDS). Fig. 1 shows the SEM pictures of the fractured cross section of pure and 21.3 wt.%GDC-impregnated LNF cathodes before Cr-poisoning test. As shown in

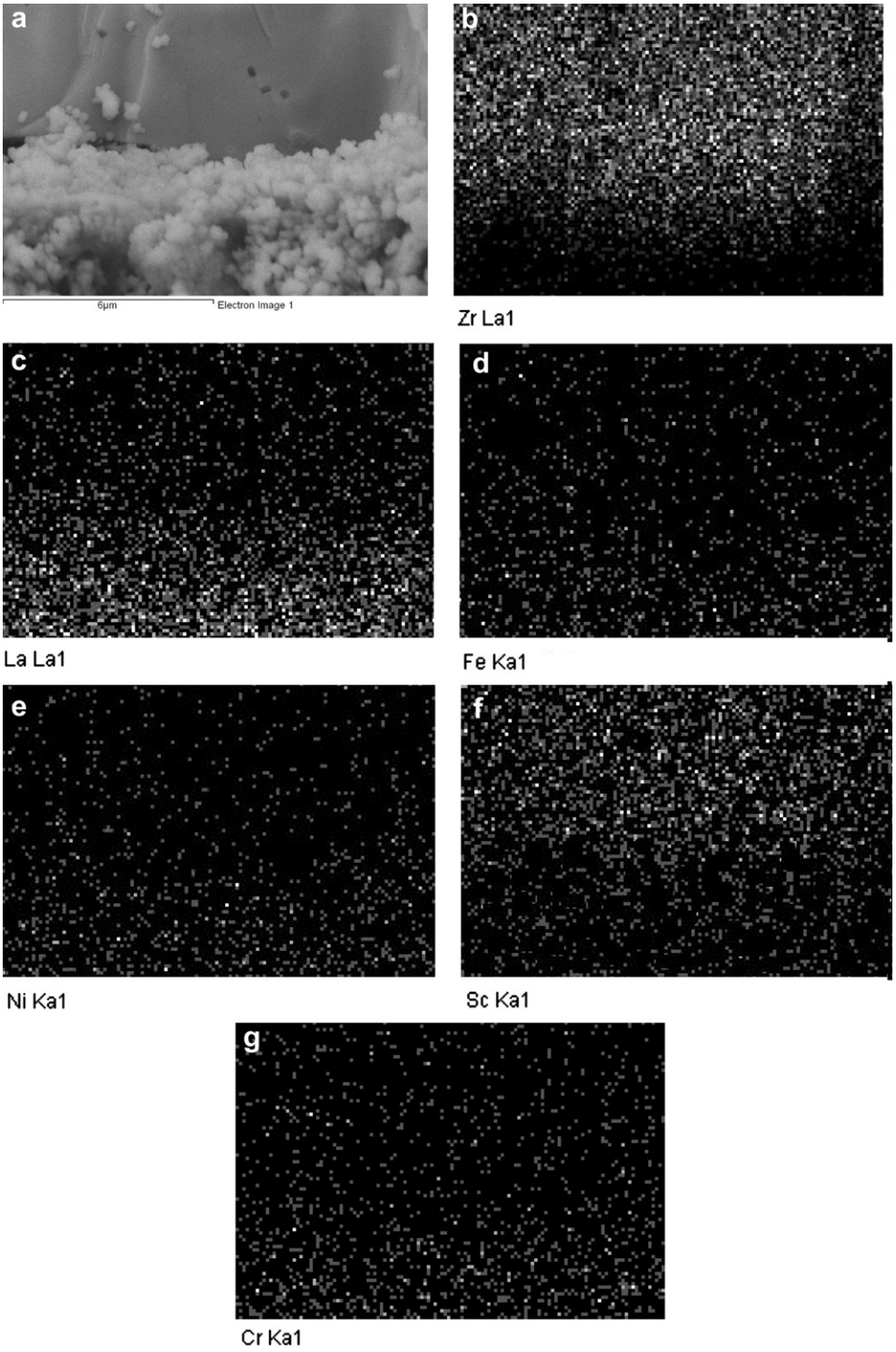

Fig. 8. Electron probe microscopic analysis (EPMA) of the LNF/ScSZ interface: (a) SEM image of the LNF/ScSZ interface; (b) Zr mapping of the interface; (c) La mapping of the interface; (d) Fe image of the interface; (e) Ni mapping of the interface; (f) Sc mapping of the interface; (g) Cr mapping of the interface. The symmetric cell was operated under a cathodic current density of 50 mA cm^{-2} under exposure of Cr vapors at 750 °C for 370 h.

Fig. 1, the microstructures of the cathodes have open pores for gas distribution. According to Ref. [40], the porosity of pure LNF cathode was 38.1% and it decreased to 6.2% for 21.3 wt.%GDC-impregnated LNF cathode. The LNF grains were in the range of 0.4–1.0 μm. After the ion impregnation with $Gd_{0.2}Ce_{0.8}(NO_3)_x$ solution, very fine particles were formed around LNF grains. The size of impregnated GDC oxide particles was in the range of 40–50 nm, as estimated from the SEM pictures. Clearly, the impregnated GDC particles are much smaller than that of LNF particles. The microstructure of 21.3 wt.%GDC-impregnated LNF cathode was characterized by the dispersion of nano-sized GDC particles in the LNF porous framework.

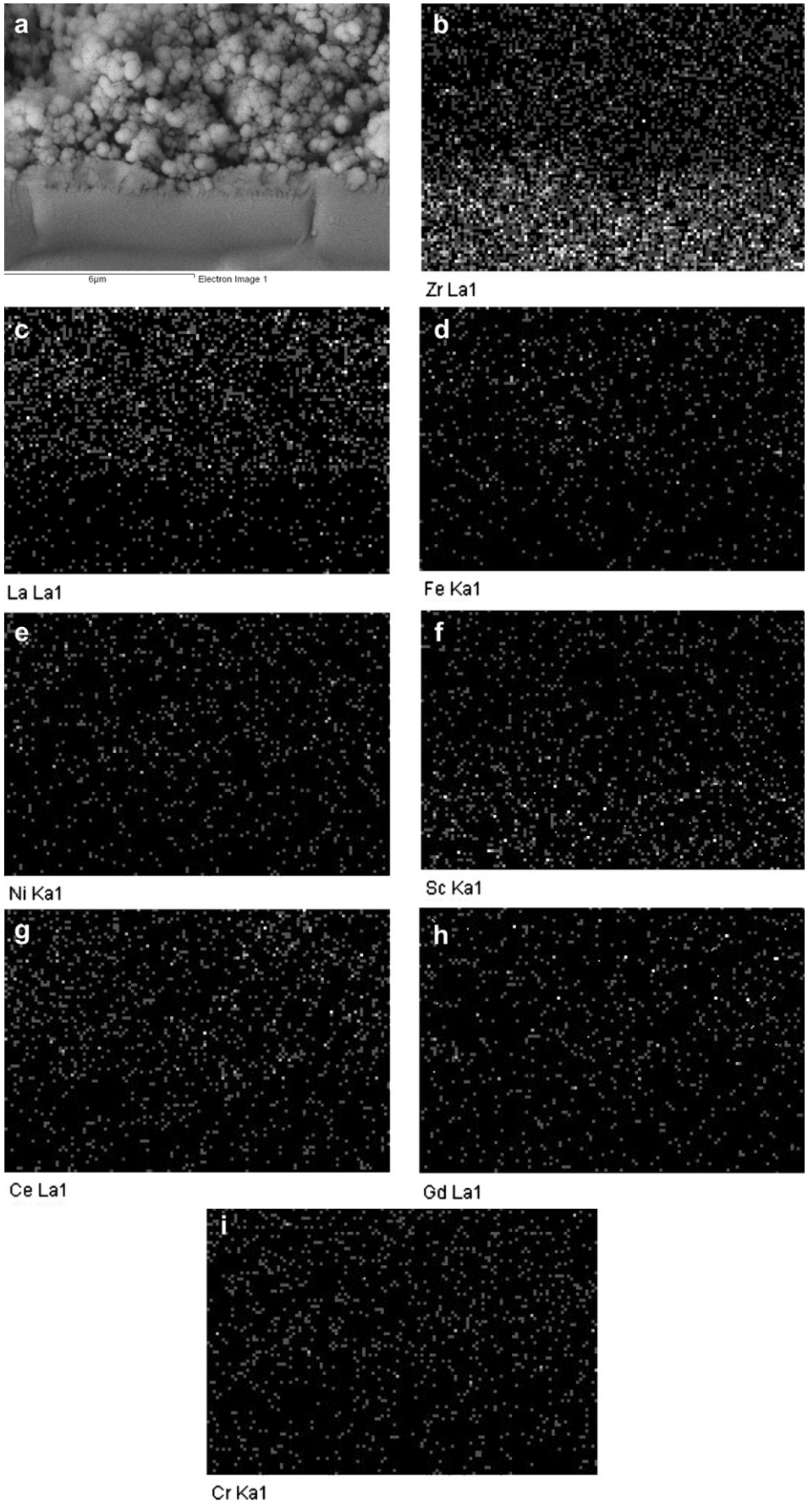
a
6μm
Electron Image 1
b
Zr La1
c
La La1
d
Fe Ka1
e
Ni Ka1
f
Sc Ka1
g
Ce La1
h
Gd La1
i
Cr Ka1

2.2. Electrochemical measurements

The electrochemical activity of the GDC-impregnated LNF cathode was characterized by the electrochemical impedance spectroscopy (EIS), using a solartron 1260 frequency response analyzer at open circuit. The applied frequency was in the range of 0.01 Hz–100 kHz at five points per frequency decade with the signal amplitude of 20 mV. The EIS measurement was carried out in the temperature range of 600–850 °C in steps of 50 °C in the air. To stabilize the cathode behavior, LNF cathodes were polarized at 750 °C with a constant current density of 50 mA cm^{-2} for 2 h before the electrochemical testing. The specific ohmic resistance (R_Ω) was estimated from the high frequency intercept of the impedance curves and the specific polarization resistance (R_p) was directly measured from the differences between the low and high frequency intercepts on the impedance curves.

In order to investigate the Cr-poisoning resistance of the GDC-impregnated LNF cathode, the long-term impedance spectra measured at 750 °C was taken. The symmetric cell in the presence of a Fe-with FECr alloy interconnect was investigated. The schematic diagram of a symmetric cell in the presence of a Fe-with FECr alloy interconnect was as follows: Fe–Cr alloy/Pt-mesh/cathode/ScSZ/cathode/Pt-mesh/Fe–Cr alloy. The cathode/ScSZ/cathode samples were set in the air atmosphere. A Pt-mesh current collector was put on the porous cathode material surface. Fe–Cr alloy (Cr_2O_3 formed on the Fe–Cr alloy surface) was placed onto the Pt-mesh current collector to avoid direct contact between Cr_2O_3 and cathodes. In this way, only Cr vapors are supplied to the cathode surface. The Fe–Cr alloy SUS 430 with 17 wt.% Cr, 1 wt.% Mn, 1 wt.% Si, 0.6 wt.% Ni, 0.12 wt.% C, 0.04 wt.% P, 0.03 wt.% S and the remaining Fe was used.

3. Results and discussion

3.1. AC impedance measurements of LNF and GDC-impregnated LNF cathodes

In an attempt to gain more information about the long-term stabilization and the degradation of LNF and GDC-impregnated LNF cathodes, we recorded the electrochemical impedance spectra of the two cathodes under a cathodic current density of 50 mA cm^{-2} without and with Cr vapors at 750 °C during the aging process. Fig. 2 depicts impedance spectra of LNF and 21.3 wt.%GDC-impregnated LNF cathodes under a cathodic current density of 50 mA cm^{-2} without Cr vapors at 750 °C during the aging process. In more detail, Figs. 3 and 4 depict consecutive impedance spectra of LNF and 21.3 wt.% GDC-impregnated LNF cathodes under a cathodic current density of 50 mA cm^{-2} under exposure of Cr vapors at 750 °C at different operating time. The spectra were analyzed by considering an R_p-Q parallel circuit with a series connection of R_Ω (R_p is the specific polarization resistance, Q is constant phase element(CPE) and R_Ω indicates the specific ohmic resistance). The high frequency intercept of the impedance spectra corresponds to the specific ohmic resistance of the symmetric cell (R_Ω), including the ohmic resistance of the ScSZ electrolyte, ohmic resistance of the cathode, contact resistance at the cathode/electrolyte interface and contact resistance between the cathodes and current collector Pt mesh. R_p is related to the cathodic polarizations associated with oxygen reduction: $O_2 + 4e^- \rightarrow 2O^{2-}$. As can be seen from Fig. 2, R_p of two kinds of cathode materials at 750 °C increased slowly with time without a significant change of R_Ω. For example, R_Ω was 0.54 and 0.48 Ω cm^2 for pure LNF cathode and 21.3 wt.% GDC-impregnated LNF cathode at 750 °C, respectively. R_Ω of pure LNF cathode under a cathodic current density of 50 mA cm^{-2} without Cr vapors at 750 °C after 370 h attained to 0.74 Ω cm^2 while that of 21.3 wt.% GDC-impregnated LNF cathode in the same conditions after 1042 h was only 0.66 Ω cm^2. R_p was 0.70 and 0.13 Ω cm^2 for pure LNF cathode and 21.3 wt.% GDC-impregnated LNF cathode at 750 °C, respectively. R_p of pure LNF cathode under a cathodic current density of 50 mA cm^{-2} without Cr vapors at 750 °C after 370 h increased almost 3.3 times (2.31 Ω cm^2) while that of 21.3 wt.% GDC-impregnated LNF cathode in the same conditions after 1042 h increased about 2.9 times (0.38 Ω cm^2). These results indicated that the impregnation of nano-sized GDC greatly accelerates the oxygen dissociation and diffusion processes. The enhancement in O_2 reduction kinetics is most likely related to the high electrocatalytic effect and the high surface areas of the impregnated nano-sized GDC phase [42]. The impregnation of the nano-sized ionic conducting GDC phase in the predominantly electronic conducting LNF porous network could substantially enhance the triple phase boundaries for the O_2 reduction. On the other hand, further investigation also suggests that the increase in R_p is mainly due to the change in the LNF cathode performance itself [43] even though it is not possible to exclude some contributions of reactions between electrolyte and cathode components, such as diffusion and/or segregation at the interface. Notably, Fe- and Ni-containing perovskites tend to lose oxygen on heating, with oxygen vacancy formation. According to Ref. [43], the increase of R_p with time could be explained by reoxidation of sintered material and consequent decrease of oxygen vacancy concentration.

Figs. 5 and 6 show the evolution of R_p and R_Ω of LNF and 21.3 wt.% GDC-impregnated LNF cathodes under a cathodic current density of 50 mA cm^{-2} under exposure of Cr vapors at 750 °C during the aging process, respectively. The variation of R_p and R_Ω with time indicated that the electrochemical reaction was not taking place under constant conditions, rather the conditions at the surface of the cathode particles and at the cathode/electrolyte interface were substantially modified with the time of coming into contact with Cr vapors. These modifications (Cr deposition at the cathode/electrolyte interface, or chemical reactivity between the LNF cathode particles and volatile Cr species) affected electrochemical performance of the cathode. The precise analysis about Cr deposition at the interface will be made soon. Further work are required to identify the stability of the LNF cathode under exposure of Cr vapors after passage of cathodic current at 750 °C with the exposure time.

As can be seen from Figs. 3–6, in case of the LNF cathode, under exposure of Cr vapors, the size of the impedance loop increased sharply with time, suggesting an increase in R_p due to the Cr deposition at the LNF/ScSZ interface. This implied that the electrochemical reaction rates associated with the cathode oxygen reduction reaction were decreasing rapidly with time. R_p of the LNF cathode under exposure of Cr vapors after passage of cathodic current at 750 °C for 370 h was 42.86 Ω cm^2, far more than that of the LNF cathode in the same condition without Cr vapors. The impedance spectra of 21.3 wt.% GDC-impregnated LNF cathode show a slow increase in R_p with operation time under exposure of Cr vapors. On one hand, it was noted that R_p of 21.3 wt.% GDC-impregnated LNF cathode under exposure of Cr vapors after passage of cathodic current at 750 °C for 1042 h was only 3.12 Ω cm^2, greater than that of the same cathode without Cr vapors

Fig. 9. Electron probe microscopic analysis (EPMA) of 21.3 wt.%GDC-impregnated LNF/ScSZ interface: (a) SEM image of 21.3 wt.%GDC-impregnated LNF/ScSZ interface; (b) Zr mapping of the interface; (c) La mapping of the interface; (d) Fe image of the interface; (e) Ni mapping of the interface; (f) Sc mapping of the interface; (g) Ce mapping of the interface; (h) Gd mapping of the interface; (i) Cr mapping of the interface. The symmetric cell was operated under a cathodic current density of 50 mA cm^{-2} under exposure of Cr vapors at 750 °C for 1042 h.

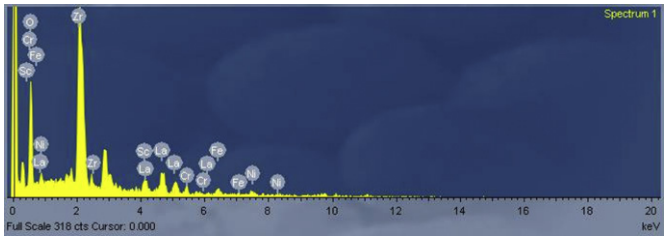

Fig. 10. EDS patterns of LNF/ScSZ interface. The symmetric cell was operated under a cathodic current density of 50 mA cm^{-2} under exposure of Cr vapors at 750 °C for 370 h.

in the same condition, but far less than that of the LNF cathode in the same condition for 370 h. On the other hand, R_Ω of 21.3 wt.% GDC-impregnated LNF cathode under exposure of Cr vapors after passage of cathodic current at 750 °C for 1042 h was only 0.96 Ω cm^2, slightly more than that of the same cathode without Cr vapors in the same condition, but significantly lower than that of the LNF cathode, which was 2.39 Ω cm^2 under exposure of Cr vapors after passage of cathodic current for only 370 h.

In this way, the Cr vapor can increase specific ohmic resistance and specific polarization resistance of the cathodes by the deposition of Cr at the cathode/electrolyte interface. R_p are plotted as a function of the operation time in Fig. 7. In the LNF cathode, the R_p values increase with time to the power of 1/3. Because the amounts of the supplied Cr vapors were proportional to the operation time, the Cr deposition at the cathode/electrolyte interface can be related to the increase in resistance. For 21.3 wt.% GDC-impregnated LNF cathode, the R_p values increase with time to the power of 1/5. By contrast, the rapid electrochemical reaction rates associated with the cathode O_2 reduction reaction on 21.3 wt.% GDC-impregnated LNF cathode was due to the cathodes employed in the symmetric cell, which combined electrically conducting phase (LNF) and oxygen ion-conducting media (nano-sized GDC). Impedance measurements taken in air for the LNF and 21.3 wt.% GDC-impregnated LNF cathodes indicate that the nano-sized GDC particles caused the specific polarization resistance to reduce by a factor of ~2. The electrocatalytic effect of the impregnated GDC on the LNF cathode behavior is indicated by the much higher tolerance of the 21.3 wt.% GDC-impregnated LNF carthode to gaseous Cr species as compared to that of the pure LNF cathode. Under a cathodic current density of 50 mA cm^{-2} at 750 °C, volatile Cr species such as $CrO_3(g)$ and $CrO_2(OH)_2(g)$ produced from chromium-based alloy can readily occupy the active sites at the LNF/ScSZ interface and effectively block the path for O_2 surface dissociation and diffusion process [44,45]. $CrO_2(OH)_2(g)$ and $CrO_3(g)$ will compete with the normal oxygen reduction process, thus Cr^{6+} can be readily reduced to Cr^{3+}, electrochemically forming Cr_2O_3 and releasing water and an oxide ion at the LNF/ScSZ interface [12], eventually resulting in the dramatically increased R_p. The much lower increase in R_p for the O_2 reduction reaction on the 21.3 wt.% GDC-impregnated LNF cathode indicates the enhanced

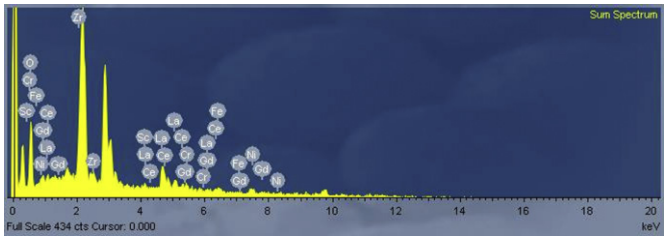

Fig. 11. EDS patterns of 21.3 wt.%GDC-impregnated LNF/ScSZ interface. The symmetric cell was operated under a cathodic current density of 50 mA cm^{-2} under exposure of Cr vapors at 750 °C for 1042 h.

bulk diffusion processes as observed on the mixed ionic and electronic conducting cathodes such as LSCF as compared to that on the dominant electronic conducting LSM and Pt electrodes [44]. Thus, GDC impregnation not only enhances the electrochemical catalytic activity of the LNF cathodes [40], but also substantially increases the bulk diffusion of oxygen in the LNF cathode and improves Cr-resistance of the LNF cathode. GDC is known to have high surface exchange properties for oxygen. Therefore, in addition to the effective electronic and ionic pathways within impregnated LNF, there might be synergistic processes involving the injection of the mobile charge oxygen surface species into the GDC ionic carrier, pointed out by Steele et al. [46]. This appears to be supported by the fact that there is significant improvement in the cathode activity for the O_2 reduction on the GDC-impregnated LNF cathodes, even though in the case of low-loading GDC (e.g., 4.7 wt.%GDC) [40], the distribution of nano-sized GDC particles seems to be isolated and there is no continuous GDC ionic conducting phase.

3.2. Microstructures of LNF and GDC-impregnated LNF cathodes

The formation of protective $Cr_2O_3(s)$ surface layers on alloys containing more than about 15 wt.% Cr (chromia-forming alloys) is well known and documented [47,48]. In the Fe–Cr alloy SUS 430, $Cr_2O_3(s)$ was formed at the surface of the Fe–Cr alloy interconnect at 750 °C. Figs. 8 and 9 show secondary electron microscopic (SEM) images and Cr mapping images of the LNF cathode and the 21.3 wt.%GDC-impregnated LNF cathode on the ScSZ electrolyte, respectively, which was operated under exposure of Cr vapors at 750 °C for 370 h and 1042 h, respectively. The porous structures were kept during the Cr exposure (Fig. 8(a) and Fig. 9(a)). Cr vapors in air were supplied inside the porous cathodes without significant microstructure change. The microstructures at the cathode/electrolyte interface show no voids and perfect adhesion of porous cathode structures on the ScSZ electrolyte.

In Fig. 8, close to the LNF/ScSZ contact interfaces, clear and strong Cr deposition (Fig. 8(g)) is observed after operating under a cathodic current density of 50 mA cm^{-2} under exposure of Cr vapors at 750 °C for 370 h and is confirmed by EDS (Fig. 10), which suggests that Cr builds up within the cathode. This may cause performance degradation shown in Fig. 3 by one or more mechanism. An observed increase in the specific ohm resistance and specific polarization resistance is typically attributed to Cr deposition at the LNF/ScSZ interface. For example, Cr deposition may block cathode pores, degrading cathode performance. Alternatively, Cr deposition may lead to volume expansion and consequent micro-cracking, presumably leading to an interruption of cathode current collection pathways. Fig. 8(a) does not show any evidence of micro-cracking, performance degradation was observed after long-term operation under a cathodic current density of 50 mA cm^{-2} under Cr deposition conditions at 750 °C. As can be seen from Fig. 9, very little Cr deposition (Fig. 9(i)) is observed in the region of the 21.3 wt.% GDC-impregnated LNF/ScSZ interface after operating under a cathodic current density of 50 mA cm^{-2} under exposure of Cr vapors at 750 °C for 1042 h and is confirmed by EDS (Fig. 11). Evidently, the intensity of Cr at the 21.3 wt.%GDC-impregnated LNF/ScSZ interface, however, is much smaller than that at the LNF/ScSZ interface, which indicates that the deposition reaction of Cr species at the former interface is kinetically slow. From these results, we find that the impregnated GDC particles can reduce Cr deposition at the LNF/ScSZ interface. It is well known that GDC is beneficial for several reasons. First, GDC-impregnated LNF cathode becomes a mixed ionic and electronic conducting conductor, a condition which should expand the reaction zone beyond three-phase boundaries. Second, the ionic conductivity of GDC is higher than that of ScSZ, which improves the transport of

oxygen ions from the cathode to the electrolyte. Third, GDC is known to readily store and transfer oxygen, and adding zirconia enhances the storage capability [49]. The 21.3 wt.%GDC-impregnated LNF cathode has additional ceria/zirconia interfaces where enhanced oxygen storage may increase cathode O_2 reduction reaction rates. Therefore, introduction of GDC into the pores of porous LNF cathode will result in a substantial increase in the ionic conductivity of the cathode and increase the triple phase boundary region expanding the number of sites available for cathode O_2 reduction reaction, therefore improve Cr-resistance of the LNF cathode. The exact reaction steps and the phase formation of the Cr deposits in the case of 21.3 wt.%GDC-impregnated LNF cathode require further study.

The most important result of the present study is the high electrochemical activity and stability of 21.3 wt.%GDC-impregnated LNF cathode for oxygen reduction despite the observed Cr deposition at 750 °C. In comparison with the reaction on the LNF cathode, R_p for oxygen reduction on the 21.3 wt.%GDC-impregnated LNF cathode is much lower. The small R_p values for the reaction at the 21.3 wt.%GDC-impregnated LNF cathode under exposure of Cr vapors also imply that the poisoning effect of Cr deposits on the reaction is very low under the conditions studied here. The results show that the 21.3 wt.%GDC-impregnated LNF cathode has a high resistance toward Cr deposition and a high tolerance toward the Cr poisoning.

However, much more work are required to clarify the effect of GDC impregnating on the resistance and tolerance toward Cr deposition and poisoning of the LNF cathode for O_2 reduction reaction, identify the chemical reactions of LNF with Cr vapors and understand the Cr deposition process on the 21.3 wt.%GDC-impregnated LNF cathode under cathodic polarization conditions with the exposure time.

4. Conclusions

Chromium poisoning and degradation are investigated at two cathodes: LNF and 21.3 wt.%GDC-impregnated LNF. R_p increases with time mainly due to the Cr deposition at the cathode/electrolyte interface. The electrochemical performance of 21.3 wt.%GDC-impregnated LNF is relatively high compared with LNF under exposure of Cr vapors due to very little Cr deposition at the 21.3 wt.%GDC- impregnated LNF/ScSZ interface. By contrast, clear and strong Cr deposition is observed at the LNF/ScSZ interfaces. Introduction of nano-sized GDC particles into the pores of porous LNF will result in a substantial increase in the ionic conductivity of the cathode and increase the triple phase boundary region expanding the number of sites available for cathode O_2 reduction reaction, therefore significantly improve the performance of LNF under exposure of Cr vapors. R_p of LNF increases with time up to 370 h to the power of 1/3, while that of 21.3 wt.%GDC-impregnated LNF increases with time up to 1042 h to the power of 1/5. Consequently, the GDC impregnating in the pores of LNF cathode makes it possible to have good stability for long-term operation under Cr exposure due to very little Cr deposition.

Acknowledgments

The authors thank the National High Technology Research and Development “863” Program of China (No.2009AA034400) and the Specialized Research Fund for the Doctoral Program of Higher Education of Ministry of Education (No.20100073120055) for the grants that support this research.

References

[1] M.C. Williams, J.P. Strakey, W.A. Surdoval, Int. J. Appl. Ceram. Technol. 2 (2005) 295.
[2] T. Kadowaki, T. Shiomitsu, E. Marsuda, H. Nakagawa, T. Tsuneizumi, T. Maruyama, Solid State Ionics 67 (1993) 65.
[3] Z. Yang, K.S. Weil, D.M. Paxton, J.W. Stevenson, J. Electrochem. Soc. 150 (2003) A1188.
[4] T. Horita, Y. Xiong, H. Kishimoto, K. Yamaji, N. Sakai, H. Yokokawa, J. Power Sources 131 (2004) 293.
[5] J.W. Fergus, Mater. Sci. Eng. A 397 (2005) 271.
[6] K. Huang, P.Y. Hou, J.B. Goodenough, Solid State Ionics 129 (2000) 237.
[7] B.J. Ingram, T.A. Cruse, M. Krumpelt, J. Electrochem. Soc. 154 (2007) B1200.
[8] K. Hilpert, D. Das, M. Miller, D.H. Peck, R. Wei, J. Electrochem. Soc. 143 (1996) 3642.
[9] M. Stanislowski, E. Wessel, K. Hilpert, T. Markus, L. Singheiser, J. Electrochem. Soc. 154 (2007) A295.
[10] D. Das, M. Miller, H. Nickel, K. Hilpert, in: U. Bossel, Druckerei J. Kinzel (Eds.), Proceedings of the First European Solid Oxide Fuel Cell Forum (3–7 October 1994, Lucerne, Switzerland), Gottingen, Germany, 1994, p. 703.
[11] H. Kurokawa, C.P. Jacobson, L.C. DeJonghe, S.J. Visco, Solid State Ionics 178 (2007) 287.
[12] S.P.S. Badwal, R. Deller, K. Foger, Y. Ramprakash, J.P. Zhang, Solid State Ionics 99 (3–4) (1997) 297.
[13] S. Taniguchi, M. Kadowaki, H. Kawamura, T. Yasuo, Y. Akiyama, Y. Miyake, T. Saitoh, J. Power Sources 55 (1995) 73.
[14] M.C. Tucker, H. Kurokawa, C.P. Jacobson, L.C. De Jonghe, S.J. Visco, J. Power Sources 160 (2006) 130.
[15] E. Konysheva, H. Penkalla, E. Wessel, J. Mertens, U. Seeling, L. Singheiser, K. Hilperta, J. Electrochem. Soc. 153 (2006) A765.
[16] H. Yokokawa, T. Horita, N. Sakai, K. Yamaji, M. Brito, Y.-P. Xiong, H. Kishimoto, Solid State Ionics 177 (2006) 3193.
[17] Di-Jia Liu, Jonathan Almer, Terry Cruse, J. Electrochem. Soc. 157 (5) (2010) B744.
[18] Teruhisa Horita, Yueping Xiong, Haruo Kishimoto, Katsuhiko Yamaji, Manuel E. Brito, Harumi Yokokawa, J. Electrochem. Soc. 157 (5) (2010) B614.
[19] S.P. Jiang, S. Zhang, Y.D. Zhen, J. Electrochem. Soc. 153 (2006) A127.
[20] S.P. Jiang, J.P. Zhang, L. Apateanu, K. Foger, J. Electrochem. Soc. 148 (2001) C447.
[21] S.P. Jiang, Y. Zhen, Solid State Ionics 179 (2008) 1459.
[22] T. Komatsu, R. Chiba, H. Arai, K. Sato, J. Power Sources 176 (2008) 132.
[23] S.P. Jiang, J.P. Zhang, X.G. Zheng, J. Euro. Ceram. Soc. 22 (2002) 361.
[24] Y. Larring, T. Norby, J. Electrochem. Soc. 147 (2000) 3251.
[25] Z. Yang, G. Xia, S.P. Simner, J.W. Stevenson, J. Electrochem. Soc. 152 (2005) A1896–A1901.
[26] X. Chen, P.Y. Hou, C.P. Jacobson, S.J. Visco, L.C. De Jonghe, Solid State Ionics 176 (2005) 425.
[27] W. Qu, L. Jian, J.M. Hill, D.G. Ivey, J. Power Sources 153 (2006) 114–124.
[28] M. Stanislowski, J. Froitzheim, L. Niewolak, W.J. Quadakkers, K. Hilpert, T. .Markus, L. Singheiser, J. Power Sources 164 (2007) 578.
[29] R. Chiba, F. Yoshimura, Y. Sakurai, Solid-State Ionics 124 (1999) 281.
[30] R. Chiba, F. Yoshimura, Y. Sakurai, Solid State Ionics 152 (2002) 575.
[31] H. Orui, K. Watanabe, R. Chiba, M. Arakawa, J. Electrochem. Soc. 151 (9) (2004) A1412.
[32] S. Li, J. Sun, X. Sun, B. Zhu, Electrochem. Solid-State Lett. 9 (2006) A86.
[33] T. Komatsu, H. Arai, R. Chiba, K. Nozawa, M. Arakawa, K. Sato, Electrochem. Solid-State Lett. 9 (2006) A9.
[34] Y.D. Zhen, A.I.Y. Tok, S.P. Jiang, F.Y.C. Boey, J. Power Sources 170 (2007) 61.
[35] G.Y. Laua, M.C. Tucker, C.P. Jacobson, S.J. Visco, S.H. Gleixner, L.C. DeJonghe, Power Sources 195 (2010) 7540.
[36] M.K. Stodolny, B.A. Boukamp, D.H.A. Blank, F.P.F. van Berkel, J. Power Sources 196 (2011) 9290.
[37] M.K. Stodolny, B.A. Boukamp, D.H.A. Blank, F.P.F. van Berkel, J. Power Sources 209 (2012) 120.
[38] F.P.F. van Berkel, M. Stodólny, M. Sillessen, J.P. . Ouweltjes, in: Proceedings of the 8th European Solid Oxide Fuel Cell Forum, European Fuel Cell Forum, vol. A0621, 2008, pp. 1–9.
[39] Jianying Chen, Shaorong Wang, Tinglian Wen, Junliang Li, J. Alloys Compounds 487 (2009) 377.
[40] Bo Huang, Xin-jian Zhu, Lv Yao, Heng Liu, J. Power Sources 209 (2012) 209.
[41] Z.P. Shao, S.M. Haile, Nature 431 (2004) 170.
[42] San Ping Jiang, Wei Wang, J. Electrochem. Soc. 152 (7) (2005) A1398.
[43] S.I. Hashimoto, K. Kammer, P.H. Larsen, F.W. Poulsen, M. Mogensen, Solid State Ionics 176 (2005) 1013.
[44] S.P. Jiang, J. Appl. Electrochem. 31 (2001) 181.
[45] S.P. Jiang, J.P. Zhang, K. Foger, J. Electrochem. Soc. 147 (2000) 3195.
[46] B.C.H. Steele, K.M. Hori, S. Uchino, Solid State Ionics 135 (2000) 445.
[47] P. Kofstad, in: High Temperature Corrosion, Elsevier Applied Science Publishers, London, 1988.
[48] W.O. Binder, in: H.H. Uhlig (Ed.), The Corrosion Handbook, John, Wiley and Sons, New York, 1966, p. 640.
[49] C.E. Hori., et al., Appl.Catal. B 16 (1998) 105.